Carbon monoxide reverses established pulmonary hypertension

Brian S. Zuckerbraun,[3] Beek Yoke Chin,[1] Barbara Wegiel,[1]
Timothy R. Billiar,[3] Eva Czsimadia,[1] Jayashree Rao,[3] Larissa Shimoda,[2]
Emeka Ifedigbo,[4] Shin Kanno,[3] and Leo E. Otterbein[1]

[1]Department of Surgery Transplant Center, Beth Israel Deaconess Medical Center, Harvard Medical School, Boston, MA 02215
[2]Department of Medicine, Johns Hopkins University School of Medicine, Baltimore, MD 21224
[3]Department of Surgery and [4]Department of Medicine, University of Pittsburgh, Pittsburgh, PA 15213

Pulmonary arterial hypertension (PAH) is an incurable disease characterized by a progressive increase in pulmonary vascular resistance leading to right heart failure. Carbon monoxide (CO) has emerged as a potently protective, homeostatic molecule that prevents the development of vascular disorders when administered prophylactically. The data presented in this paper demonstrate that CO can also act as a therapeutic (i.e., where exposure to CO is initiated after pathology is established). In three rodent models of PAH, a 1 hour/day exposure to CO reverses established PAH and right ventricular hypertrophy, restoring right ventricular and pulmonary arterial pressures, as well as the pulmonary vascular architecture, to near normal. The ability of CO to reverse PAH requires functional endothelial nitric oxide synthase (eNOS/NOS3) and NO generation, as indicated by the inability of CO to reverse chronic hypoxia–induced PAH in eNOS-deficient $(nos3^{-/-})$ mice versus wild-type mice. The restorative function of CO was associated with a simultaneous increase in apoptosis and decrease in cellular proliferation of vascular smooth muscle cells, which was regulated in part by the endothelial cells in the hypertrophied vessels. In conclusion, these data demonstrate that CO reverses established PAH dependent on NO generation supporting the use of CO clinically to treat pulmonary hypertension.

CORRESPONDENCE
Leo E. Otterbein:
lotterbe@bidmc.harvard.edu

Abbreviations used: eNOS, endothelial NOS; FHH, fawn-hooded hypertensive; HO-1, heme oxygenase–1; HPF, high power field; HRP, horseradish peroxidase; iNOS, inducible NOS; IVS, intraventricular septum; MCT, monocrotaline sodium; mPAP, mean pulmonary arterial pressure; mRVP, mean right ventricular pressure; NO, nitric oxide; NOS, NO synthase; PAEC, pulmonary artery endothelial cell; PAH, pulmonary arterial hypertension; PAVSM, pulmonary artery vascular smooth muscle; PI, propidium iodide; RV and LV, right and left ventricle, respectively; RVH, right ventricular hypertrophy; TUNEL, Tdt-mediated dUTP-biotin nick-end labeling.

Pulmonary arterial hypertension (PAH) is a disease of the small pulmonary arteries that is characterized by vascular proliferation and remodeling, with progressive increases in pulmonary vascular resistance leading to right heart failure and, ultimately, death (1, 2). Although PAH may be idiopathic, familial, or secondary to multiple distinct diseases, there are common pathophysiological features, including remodeling of the pulmonary vessel wall, vasoconstriction, and thrombosis (3). The cellular and molecular events underlying the evolution of these changes are under investigation and continue to guide the development of potential therapeutics (4, 5). A substantial number of molecules and molecular pathways have been implicated. Impaired production of vasoactive nitric oxide (NO) or prostacyclins, or overexpression of vasoconstrictors such as endothelin-1 can alter pulmonary vascular tone and lead to vascular remodeling (6–9). Alterations in these vasoactive molecules suggest that endothelial dysfunction plays a key role.

Previous experiments have illustrated that induced expression of heme oxygenase–1 (HO-1; the gene is referred to as *hmox-1*), the inducible heme-degrading enzyme, given before the disease-causing stimulus is protective against the development of PAH. Induction of HO-1 protects against vascular remodeling and the development of PAH in chronic hypoxia in rats, and *hmox-1$^{-/-}$* mice exhibit an exaggerated response to chronic hypoxia compared with wild-type mice (10, 11). The mechanism by which HO-1 induction can prevent PAH has been elusive. Insight, however, was garnered by Minamino et al., who showed that transgenic mice that overexpress HO-1 in a small population of epithelial cells of the lung were protected against pulmonary inflammation, PAH, and vessel wall hypertrophy in response to hypoxia (12). These data strongly suggest that a soluble mediator generated by HO-1 mediated the protection afforded in the pulmonary vasculature. The gaseous molecule carbon monoxide (CO), which arises
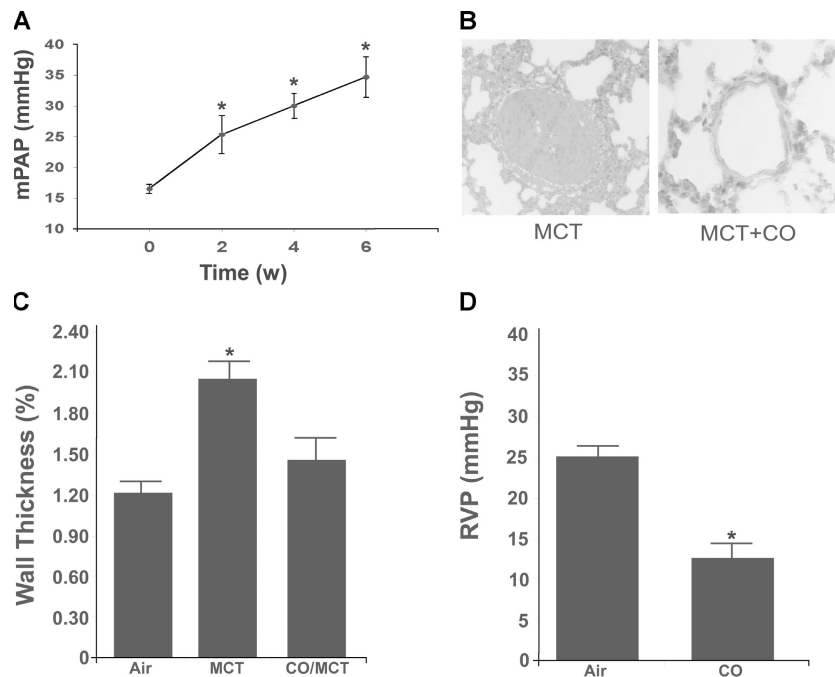
Figure 1. CO protects against and reverses MCT–induced experi–mental PAH in rats. (A) Kinetics demonstrating increasing mPAP at 2, 4, and 6 wk after a single s.c. injection of MCT on day 0. Results represent means $\pm$ SD of six to eight rats/group. *, P < 0.02 versus untreated rats. (B) Representative histological specimen of pulmonary arteriole 6 wk after MCT treatment with and without exposure to 250 ppm CO on days 29–42. Note that MCT increases medial expansion without thrombosis, whereas those animals treated with CO showed considerably reduced vascular hyperplasia. Images are representative of six to eight sections/lung from four to six rats. (C) CO reverses MCT-induced pulmonary arteriolar thick-ening in rats treated with CO on days 29–42 after MCT. Data are presented as percent wall thickness calculated as the area bounded by the internal and external laminae (see Materials and methods). Results represent means $\pm$ SD of 10 vessels from the lungs of five rats/group. *, P < 0.02 versus CO and CO/MCT. (D) In the genetically predisposed FHH rats, a sig-nificant reduction in mean RV pressures (which is reflective of mPAP) was observed in those animals treated with CO. Results represent means $\pm$ SD of four to six rats/group. *, P < 0.01 versus air- and CO-treated rats.

endogenously from all cells via the catabolism of heme by the heme oxygenase enzymes, possesses salutary actions in numerous disease models when administered exogenously at low, nontoxic concentrations (13). We and others have previously demonstrated that CO substantially diminishes vascular intimal hyperplasia after direct mechanical and trans-plant-related immunological injuries, as well as hypoxia-

induced PAH (14–17). In these injury models, inhaled CO was administered before the development of vascular injury. The effects of CO in these models have been attributed to both cyclic guanosine 3′,5′-monophosphate–dependent and –independent modes of action. Moreover, studies have dem-onstrated that CO derived from heme oxygenase expression may mediate decreased pulmonary artery vascular resistance

Table I. Effect of CO on MCT-induced changes in body weights, cardiac weights, and pulmonary hemodynamics in rats

	No MCT		MCT			
	Air	CO	Air	CO (days 1–14)	CO (days 15–28)	CO (days 29–42)
Number (n)	6	6	8	6	6	9
BW (g)	288 $\pm$ 31	291 $\pm$ 37	249 $\pm$ 52	303 $\pm$ 56	296 $\pm$ 53	301 $\pm$ 70
mPAP (mmHg)	15.8 $\pm$ 0.75	16.1 $\pm$ 1.0	34.6 $\pm$ 2.8#	15 $\pm$ 2*	19.8 $\pm$ 2.7*	21.1 $\pm$ 4.0*
RV mass (mg)	143 $\pm$ 21	137 $\pm$ 19	414 $\pm$ 27#	165 $\pm$ 21*	207 $\pm$ 51*	214 $\pm$ 59*
LV + IVS (mg)	524 $\pm$ 29	530 $\pm$ 33	696 $\pm$ 15	617 $\pm$ 178	639 $\pm$ 196	690 $\pm$ 156
RV/BW	0.49 $\pm$ 0.01	0.47 $\pm$ 0.04	1.66 $\pm$ 0.15#	0.54 $\pm$ 0.06*	0.69 $\pm$ 0.1*	0.71 $\pm$ 0.2*
RV/LV + IVS	0.26 $\pm$ 0.01	0.26 $\pm$ 0.03	0.60 $\pm$ 0.05#	0.28 $\pm$ 0.05*	0.33 $\pm$ 0.06*	0.31 $\pm$ 0.07*

PAH was assessed on day 43 following MCT treatment. MCT induced significant PAH (air vs. no MCT) as assayed by mPAP, RV mass, and the ratios of RV/BW and RV/LV + IVS. CO treatment, when started on days 1–14, 15–28, or 29–42, prevented or reversed MCT-induced changes in the heart and lung parameters listed. n = number of animals/group. #, P < 0.01 versus no MCT; and *, P < 0.01 versus air + MCT. BW, body weight.

and inhibit hypoxic vasoconstriction (18–20). CO also exerts potent antiinflammatory effects, inhibits platelet aggregation, and can be pro- or antiapoptotic depending on the cell type (16, 21). There is no information whether CO might act therapeutically to treat and modulate established PAH.

We hypothesized that CO treatment would ameliorate and reverse PAH even when given after PAH pathology has been established (i.e., as a therapeutic that is therefore clinically relevant). There is one published study demonstrating that inhaled CO can prevent the development of hypertension (17), but in that study CO was administered continuously and initiated at the time of hypoxia, which clinically is not relevant. Our data in this paper would offer a potential approach that could be tested in the clinical setting, where pretreatment is not an option. We therefore designed our treatment regimens based on this premise, using three well-established models of PAH in rodents. Although these are well characterized and accepted models of hypertension, complete extrapolation to human disease remains limited.

RESULTS
CO reverses pulmonary hypertension in rats
Monocrotaline sodium (MCT), chronic hypoxia, and the genetically susceptible fawn-hooded hypertensive (FHH) rat strains were used to evaluate the effects of CO on PAH. Exposure to CO at 250 ppm for 1 h increases COHb to ∼19%, which correlates to the accepted Coburn computation for this exposure regimen (18). The COHb levels return to baseline (<1%) within 3–4 h after discontinuing CO. In the MCT model, the development of PAH was examined at 2, 4, and 6 wk after MCT treatment (Fig. 1 A). The development of PAH was progressive, and by 2 wk MCT induced significant (P < 0.02) PAH as determined by the mean pulmonary arterial pressure (mPAP), right ventricle (RV)/left ventricle (LV) + intraventricular septum (IVS) mass ratio and the RV/body mass ratio. These data show that there is significant PAH established by 2 wk after MCT and allow us to determine if CO can act as a therapeutic to reverse established PAH.

We tested various times after the start of MCT treatment to begin CO administration. Our first experiments tested CO administration starting only 1 d after MCT. 250 ppm CO was delivered as an inhaled gas for 1 h/d on days 0–14 (after MCT administration) of the experiment. PAH was assessed at 6 wk. This early pretreatment regimen of CO prevented the development of PAH (Table I). We next extended the time course to evaluate the effects of CO when delivered only on days 15–28 or days 29–42 after starting MCT, time points at which there were already cardiopulmonary pathophysiologic changes associated with PAH. CO treatment on days 15–28 or 29–42 significantly reversed mPAP and prevented further progression of PAH based on the RV/LV + IVS and RV/body mass ratios (P < 0.01; Table I). Additionally, histological analyses showed a considerable reduction in pulmonary arterial hyperplasia, as evident by increased medial expansion of the smooth muscle cells. (Fig. 1 B). Vascular

morphometric measurements of the smaller pulmonary arteriolar changes induced in response to MCT showed the well-described increase in medial wall thickness and lumen (wall ratios further characterizing the injury are shown in Fig. 1 C). Exposure to CO on days 29–42 showed a significant reduction of wall thickness from 2.1 ± 0.09 to 1.4 ± 0.1 (P < 0.01), supporting the findings in mPAP and right ventricular hypertrophy (RVH). Determination of COHb levels in rats exposed to 1 h of CO at 250 ppm reached a concentration of 19 ± 1.5% from baseline concentrations of 1.2 ± 0.5% (P < 0.001) and returned to baseline within 4–6 h, which is expected based on standard Coburn calculations.

To corroborate and support the findings with MCT, we used two additional well-described models of PAH in rats:
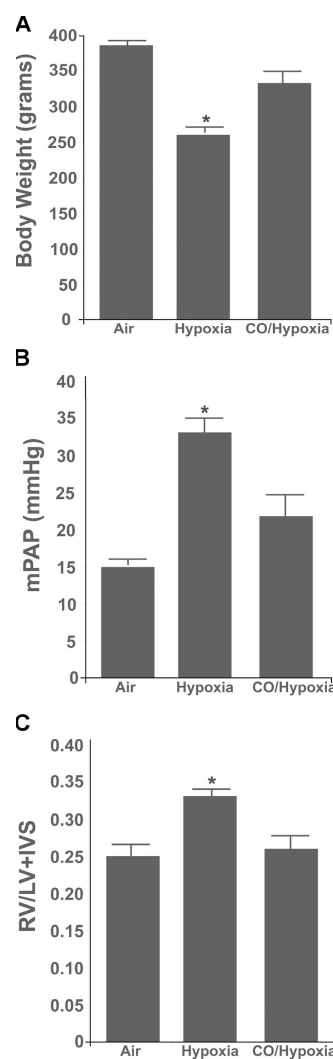

Figure 2.   CO protects against and reverses chronic hypoxia–induced experimental PAH in rats. (A–C) CO reverses pathology associated with chronic hypoxia-induced PAH, including restoring body weights (A) and lowering hypoxia-induced increases in mPAP (B), as well as RV/LV + IVS ratios (C). Results represent means ± SD of six rats/group. *, P < 0.01 versus CO/hypoxia- and air-treated controls.

the chronic hypoxia–exposed rat and the FHH rat, which is genetically predisposed to the development of PAH and its pathology by 12–16 wk of life in the absence of hypoxia. A similar exposure regimen was implemented in these two models. CO exposure of the FHH rats was begun at 12 wk of age, when there was a significant increase in right ventricular pressure that resolved to near normal in response to CO (24 ± 1.7 mmHg in air vs. 12 ± 1 mmHg in CO–treated animals; $P < 0.01$; Fig. 1 D). In the hypoxia model, rats were exposed to 10% O_2 for 6 wk. 3 wk from the start of the expo-

sure, at which point PAH is well established, the CO exposure regimen (250 ppm for 1 h/d) was implemented for the additional 3 wk. After each daily 1-h exposure to CO, the rats were returned to hypoxic conditions. Control animals were removed and exposed to room air for the 1-h period and then returned to hypoxia. Chronic exposure to hypoxia leads to a decrease in body weight with time. An initial indication of the beneficial effects of CO administration was observed here with an increase in body weights compared with untreated hypoxia/air controls ($P < 0.01$; Fig. 2 A).
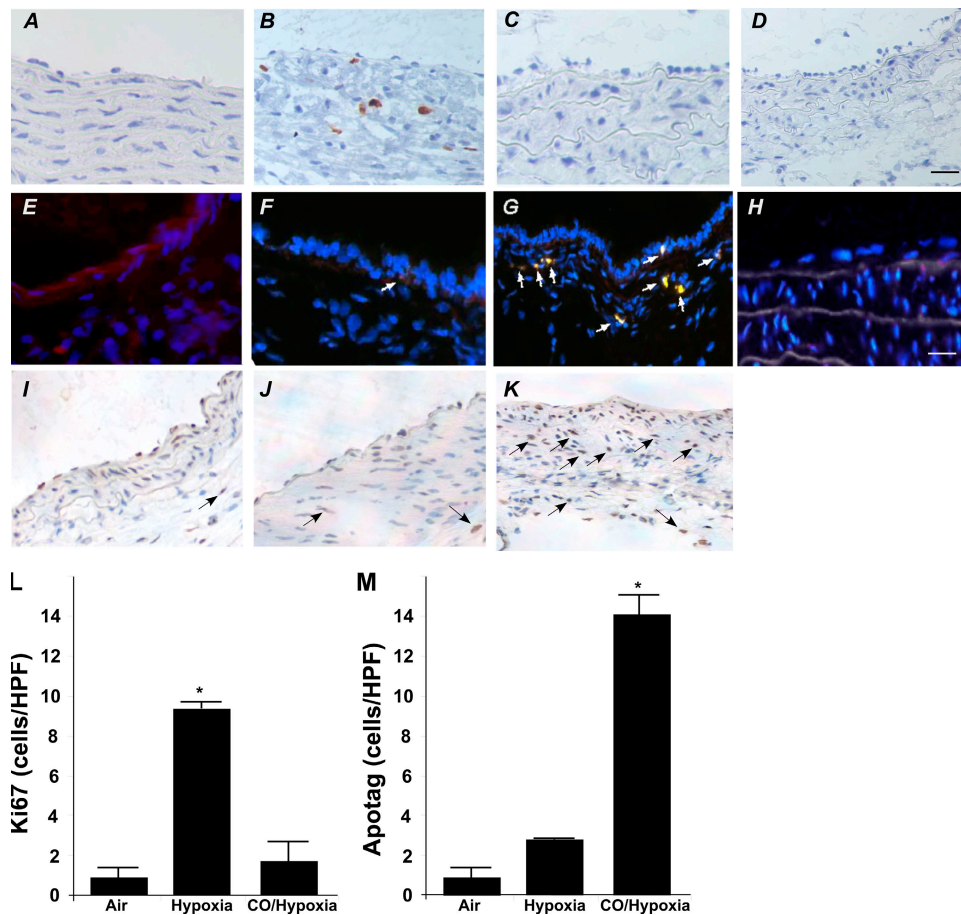

Figure 3.   CO ameliorates MCT–induced PAH via blocking proliferation and increasing apoptosis of the vascular smooth muscle cells in the pulmonary artery. Lungs from rats treated with MCT in the presence and absence of 250 ppm CO for 1 h/d (initiated 3 wk after induction of PAH) were harvested on day 43, fixed, sectioned, and stained for markers of proliferation and apoptosis. The majority of positive staining colocalized to smooth muscle cells. Vascular smooth muscle cell proliferation, as determined by Ki67 immunostaining, was not present in untreated animals (A), but it was increased in hypoxia- and MCT-induced PAH (hypoxia is shown; B) and substantially decreased by CO treatment (C). Images are representative of six to eight sections/lung from four to six rats/group. Cellular apoptosis, as determined by TUNEL staining, is absent in untreated and hypoxia-treated rats (E and F, respectively); however, sections from chronic hypoxia-treated animals treated with CO for 1 h/d resulted in a considerable increase in TUNEL-positive smooth muscle cells (G). The arrows in F and G represent positively stained cells. (I–K) Representative images from the same animals as above (E–G), immunostained for activated caspase-3. Arrows designate positive peroxidase staining. Note that the relative number of caspase-3–positive cells (I–K) correlates with the percentage staining positive for apoptotic cells (E–G). Additionally, in contrast to the proliferation staining whereby CO was inhibitory, CO increased positive staining for cell death and activated caspase-3 and simultaneously decreased tissue mass. This offers one explanation as to the mechanism by which restoration of normal pulmonary arterial pressure and RV mass occurs. Quantitation of the positively stained cells for Ki67 and Apotag/TUNEL are shown (L and M, respectively). (D and H) Negative control stainings for peroxidase and fluorescent images. The same secondary anti-HRP antibody was used for both Ki67 and caspase-3. All images are representative of six to eight sections/lung from four to six rats/group. Histograms represent means $\pm$ SD of positively stained cells from 15–20 fields. *, $P < 0.01$ versus air- or hypoxia-treated rats. Bar, 10 μm.
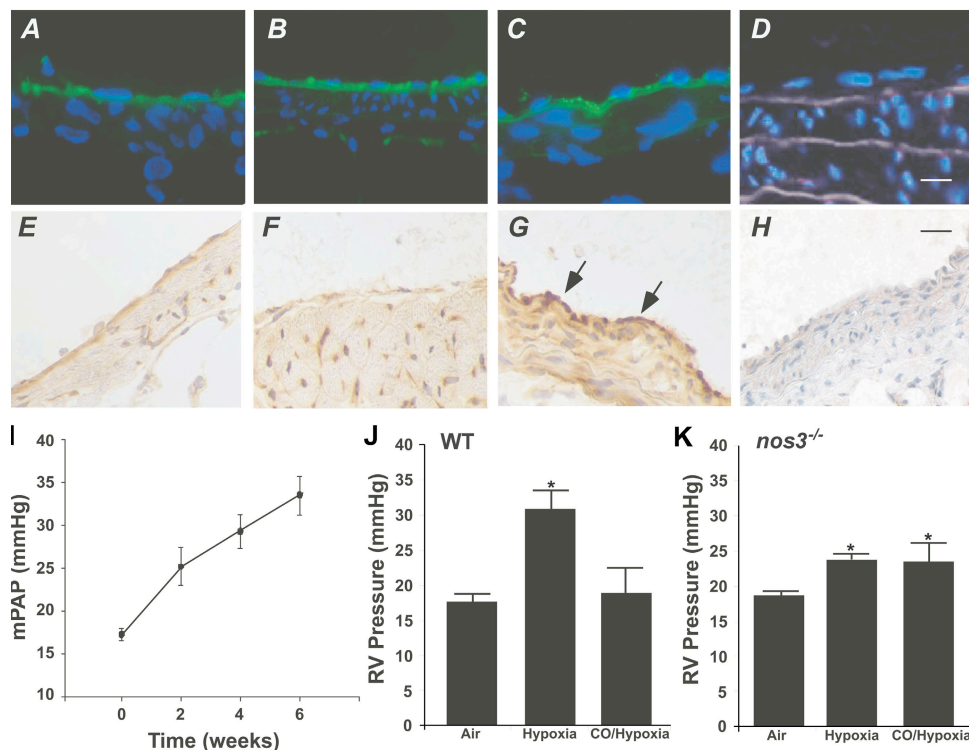
Figure 4. CO increases eNOS expression in PAECs, which is required for CO to reverse PAH in chronic hypoxia–exposed animals. (A–C) Lungs from rats chronically exposed to air (A), hypoxia (B), or hypoxia plus 250 ppm CO for 1 h/d (C) as described in Fig. 6. Lung sections were then stained with CD31 (green) to identify PAECs in larger arterioles. None of the treatment regimens resulted in a change in CD31 staining or morphology, nor were there alterations in PAEC numbers. (E–G) Sections from the same lung preparations as above (A–C) stained for eNOS expression. Only those animals treated with hypoxia in the presence of CO (G) showed a substantial increase in eNOS expression, which was not otherwise modulated in air- and hypoxia-treated animals (E and F, respectively). eNOS-positive staining in the endothelial cell is denoted by arrows. There is a trend toward less eNOS positivity in the endothelium of hypoxia-treated animals, which is consistent with a published report (reference 30). Images are representative of six to eight sections/lung from four to six rats/group. D and H show secondary antibody negative control images. Bar, 10 μm. (I) Mice exposed to chronic hypoxia develop a time-dependent increase in mPAP, as expected. Wild-type and $nos3^{-/-}$ mice (J and K) were exposed to either chronic hypoxia or chronic hypoxia plus CO using the same protocol as described for the rats (see Fig. 6). We observed an increase in RV pressure in wild-type mice exposed to chronic hypoxia, which was reversed by CO (J). In the $nos3^{-/-}$ mice, there was a more modest, but significant, increase in mean RV pressure. CO was unable to reverse this increase in PAH in $nos3^{-/-}$ mice (K). Results represent means $\pm$ SD from four to six mice/group. *, P < 0.01 versus air controls.

Increased mPAP developed in hypoxic animals at 6 wk, as indicated by an elevated mPAP of 30 mmHg compared with 16 mmHg in untreated rats. There was also a corresponding 30% increase in the RV/LV + IVS ratio (0.35 $\pm$ 0.2 in hypoxia-treated rats vs. 0.25 $\pm$ 0.25 in control rats; P < 0.01; Fig. 2, B and C). In contrast, animals that were treated with CO showed a restoration of mPAP, RV/LV + IVS ratios similar to those found in untreated wild-type rats (20 $\pm$ 4 mmHg and 0.26 $\pm$ 0.4, respectively; Fig. 2, B and C).

CO promotes negative pulmonary vascular remodeling
To reverse vascular hyperplasia and improve PAH, there must be a net loss in the cellular mass of the vessel wall and the underlying smooth muscle cells. This can occur via decreased proliferation and/or increased cell death. An apoptotic index was determined using Tdt-mediated dUTP-biotin nick-end labeling (TUNEL) staining of the pulmonary arterial wall in both the hypoxia and MCT experimental groups while proliferation was simultaneously assessed in similar sections by immunostaining for Ki67. The number of positively stained cells was enumerated by a blind experimental protocol. In both the hypoxia-treated group (Fig. 3) and in the MCT animals (not depicted), we observed elevated Ki67-positive staining in the smaller arterioles that was markedly reduced in the vessels of rats exposed to CO (9 $\pm$ 3 vs. 0.5 $\pm$ 0.5 cells/high power field [HPF], respectively; P < 0.01; Fig. 3, A–C and J). The opposite effect was observed in assessing the degree of cell death in the pulmonary arterial wall. There was a marked elevation in the number of apoptotic-positive cells in the CO-treated rats versus the number present in the MCT- or hypoxia-treated controls (19 $\pm$ 3 vs. 2 $\pm$ 1 cells/ HPF [MCT] and 14 $\pm$ 2 vs. 4 $\pm$ 3 [hypoxia]; P < 0.01 for both; Fig. 3, D–F and K). Confirmatory immunostaining for caspase 3 (Fig. 3, I–K) showed a similar pattern as that observed with TUNEL (Fig. 3, E–G). CO increased the number of caspase 3–positive cells in the arterial wall of chronic
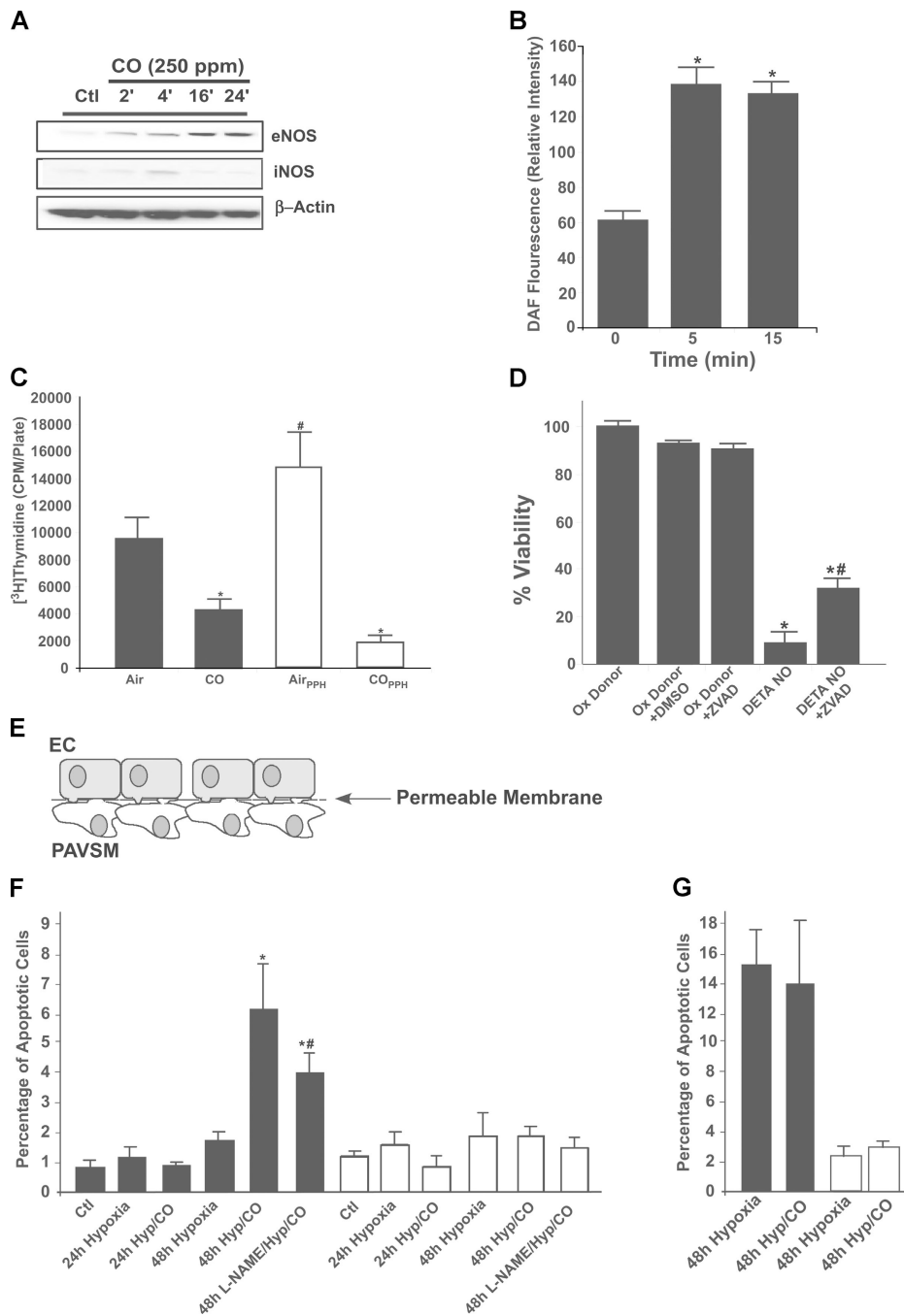
Figure 5. Interrelationship between CO and NO on endothelial cells and PAVSM cells. (A) Kinetics of eNOS and iNOS expression in PAECS. Western blot from PAECS exposed to 250 ppm CO shows a time-dependent increase in eNOS, but not iNOS, expression. β-actin is shown as a loading control. Blots are representative of four independent experiments. (B) CO increases NO generation in PAECs. PAECs exposed to CO and measured NO production by the changes in DAF fluorescence are shown. CO increased DAF fluorescence as early as 5–15 min. Means ± SD of triplicate wells from six to eight independent experiments are given. *, P < 0.01 versus time 0. (C) Effects of CO on PAVSM cell proliferation. PAVSM cells from rats (shaded bars) or freshly isolated human PAVSM cells from an individual with primary pulmonary hypertension (open bars) were exposed to CO, and proliferation was assessed by thymidine incor-

poration. Note that CO induced growth arrest in both cell types. Results represent means ± SD of triplicate wells from three independent experiments. *, P < 0.001 versus air-treated rats. (D) NO induces cell death in PAVSM cells. Rat PAVSM cells were treated with 500 μM of the NO donor DETA-NONOate for 36 h, and cell viability was assessed by crystal violet. Note that DETA-NONOate–induced cell death was reversed in part by treatment with the pancaspase inhibitor ZVAD-fmk. Results represent means ± SD of triplicate samples from two independent experiments. *, P < 0.001 versus controls; and #, P < 0.05 versus DETA-NONOate–treated samples. (E) The co-culture schematic is a diagram demonstrating the co-culture system that allows cell–cell contact. Cells were seeded and treated as described in Materials and methods. (F) PAECs and PAVSM cells were co-cultured and exposed to control conditions (5% CO$_2$ ± CO),

hypoxia- exposed rats with similar quantitative changes as seen in the TUNEL-stained tissue (unpublished data).

CO reversal of PAH requires endothelial NO synthase (eNOS) expression

We probed whether negative remodeling in CO-treated animals was occurring as a result of an increased production of the vasoregulatory molecule NO. Immunohistochemistry for CD31 demonstrated no substantial quantitative difference in endothelial cells in hypoxia as compared with the CO-/hypoxia-treated groups (Fig. 4, A–C). However, staining for eNOS (NOS3) showed a marked increase in expression in the CO-/hypoxia-treated rats (Fig. 4, E–G). To test whether CO required eNOS expression/activation, we exposed wild-type C57BL/6 and $nos3^{-/-}$ C57BL/6 mice to chronic hypoxia. This is a reliable and well-characterized model of PAH that has identical kinetics as in the rat. Fig. 4 I shows the kinetic development of PAH in mice exposed to chronic hypoxia. C57BL/6 mice were randomized to groups comprising chronic hypoxia treatment with a 1 h/d exposure to 250 ppm CO or room air. Mice were exposed to 10% oxygen continuously for 42 d. Mice were treated only during days 22–42 with inhaled CO (250 ppm for 1h/day) or air. As in the rat, significant improvement in mean right ventricular pressure (mRVP) was evidenced in the CO-treated group (P < 0.05; Fig. 4 J). To evaluate the contribution of eNOS to the protective effects of CO, the wild-type and $nos3^{-/-}$ mice were exposed to chronic hypoxia for 42 d and either not treated or treated with CO on days 22–42. Although CO effectively reversed the mRVP in wild-type mice (22 ± 3; P < 0.01), it was unable to reverse hypoxia–induced PAH in $nos3^{-/-}$ mice (Fig. 4 K). These data implicate eNOS and NO in the protection afforded by CO in restoring normotensive pulmonary arterial pressures.

CO increases eNOS expression in pulmonary artery endothelial cells (PAECs)

We found that CO has the same action in vitro as in vivo: it stimulates increased protein levels of eNOS in PAECs (Fig. 5 A). These cells did not demonstrate increased inducible NOS (iNOS) protein in response to CO and, thus, we did not test further the role of iNOS in this model. Moreover, using FACS analyses, PAECS treated with CO demonstrated a rapid increase in DAF fluorescence, an indicator of NO generation (Fig. 5 B). This response is not likely caused by increased levels of eNOS protein but could result from functional changes in NOS activity or increased liberation of NO from within the cell.

NO increases caspase–dependent cell death of pulmonary artery smooth muscle (PAVSM) cells

We next tested whether NO might increase cell death of PAVSM cells in vitro. We observed a significant decrease in PAVSM cell proliferation in response to CO in both rat PAVSM cells and fresh human PAVSM cells isolated from a patient with pulmonary hypertension (P < 0.001; Fig. 5 C). We next exposed primary rat PAVSM cells to increasing doses (10–500 μM) of the NO donor, DETA-NONOate, and measured the number of viable cells by crystal violet staining. To differentiate decreased proliferation from increased apoptosis, we examined the effects of DETA-NONOate (500μM) on PAVSM cells in the presence of the pancaspase inhibitor zVAD-fmk (50 μM). NO significantly decreased cell viability and crystal violet staining. This effect was abrogated by the addition of zVAD, suggesting that, at least in part, NO functions by inducing apoptosis in PAVSM cells (P < 0.05; Fig. 5 D).

CO–induced PAVSM cell death is dependent on the presence of PAEC and NO generation

Using a co-culture system in which PAVSM cells and PAECs were grown on either side of a semipermeable membrane with direct physical access to one another (see Fig. 5 E), we evaluated whether exposure to hypoxia in the presence of CO would modulate the susceptibility of the PAVSM cells to cell death without affecting the PAECS and thereby provide a mechanism by which CO exerted its effects in vivo in the pulmonary vasculature. Using FACS analyses of propidium iodide (PI) as a marker of cell viability, we exposed the co-cultured cells to hypoxia or hypoxia plus 250 ppm CO and harvested the cells at 24 and 48 h. At the designated time points, each cell type was harvested separately to avoid contamination, prepared as described in Materials and methods, and a FACS analysis was performed. Exposure of the co-cultures to 1% O_2, air, or CO alone had no effect on PAVSM cell or PAEC viability, showing no change in PI incorporation. In contrast, when the cells were exposed to 1% O_2 plus 250 ppm CO for 48 h, there was a marked increase in PI staining of the PAVSM cells, increasing greater than fivefold versus hypoxia alone–treated cells, which was indicative of increased cell death. Importantly, there was no observed change in viability of the PAECs harvested from any exposure regimen (Fig. 5 F). No changes in PI staining were observed in any treatment group at 24 h.

We conclude that co-culturing and allowing these two cell types to interdigitate while being exposed to these regimens leads to the ability of these cells to more closely

---

hypoxia, or hypoxia plus CO for 24 and 48 h, and cell viability was determined by FACS analyses of PI staining, as described in Materials and methods. Inclusion of CO in the hypoxia exposure resulted in an increase in cell death selectively in PAVSM cells (shaded bars) but not PAECs (open bars). Blockade of NOS using L-NAME in the co-culture system reversed the effect of CO on cell death. PAECs were unaffected in all treatment groups. Results represent means ± SD of six wells/group from two independent co-culture experiments. *, P < 0.01 versus control and non-CO–treated cells; and #, P < 0.03 versus hypoxia-/CO-treated cells. (G) CO is unable to increase PAVSM cell death. PAVSM cells (shaded bars) and PAECs (open bars) grown in standard non–co-culture systems and exposed to CO showed no differences in cell death. Means ± SD are shown.

communicate and thereby mimic the proximity of these cells to one another in the in vivo setting. One such mediator for which this would be important is NO, which, being highly reactive, would most likely not exist in sufficient quantities to allow communication in a standard co-culture system where there is typically a media gap between cell types. To test the role of NO in the observed effect with CO in this co-culture system, we exposed cells to identical treatments in the presence and absence of the NOS inhibitor L-NAME. Co-cultures were treated with 250–500 μM L-NAME 1 h before exposure. Blockade of NOS in the co-culture system led to a reversal of hypoxia plus CO-induced PAVSM cell death assessed by PI staining, with no effects on the PAECS (Fig. 5 F). L-NAME alone had no effect on viability in nonhypoxia plus CO-treated cells (not depicted).

To address the relevance and importance of co-culture experiments, we exposed monolayers of each cell type in standard cell culture dishes to identical treatment regimens of hypoxia and CO and observed no change in cell death among groups (Fig. 5 G).

DISCUSSION

These results demonstrate that daily exposure to a low concentration of CO for 1 h can reverse established PAH in rodents, suggesting the potential for a novel and practical therapeutic option in the treatment of this devastating disease, keeping in mind the necessary caution when extrapolating from animal models to the clinical setting. Nevertheless, these three models provide strong evidence to approach clinical testing. *hmox-1*, the gene responsible for endogenous CO generation, is highly induced in patients and rodents with PAH, which is indicative of its importance as a stress response protein (16, 19–24). Induction of HO-1 before the disease process starts can ameliorate development of PAH and RVH (11). Inducing HO-1 therapeutically (i.e., after the PAH disease process has started) has not been tested. Heme oxygenase activity results in the generation of three products: the bile pigments, iron, and CO. The bile pigments, as well as the sequestration of iron into ferritin, have been shown to impart potent antioxidant effects. We hypothesized that CO could substitute for the effects of HO-1 and might serve to alleviate PAH even as a treatment after the disease process has started. It is possible, but outside the scope of this study, that biliverdin and ferritin administration might impart additional or additive effects otherwise observed with HO-1 induction and, moreover, exert protective effects via separate and distinct mechanisms.

In three separate rodent models, we demonstrate that CO can reverse established PAH, reduce right heart mass, and improve overall health of the animal, as indicated by improved body weight. We did not measure the effects of CO on metabolic rate or food intake, which might be altered, as well as altered regulation of leptin expression. In the mouse chronic hypoxia model, these effects require the expression of eNOS and the generation of NO. Whether a similar requirement exists for the other models of PAH is not yet known. Decreased eNOS expression has been demonstrated

in endothelial cells from PAH patients (6). Previous experiments have shown that mice with targeted disruption of the eNOS gene exhibit increased mPAP and impaired vasorelaxation in response to acetylcholine (25). In our experiments, the $nos3^{-/-}$ mice did not demonstrate as great an increase in mRVP in response to hypoxia as previously published (25) when compared with wild-type mice (29 ± 5 mmHg in C57BL/6 hypoxic mice vs. 25 ± 1 mmHg in $nos3^{-/-}$ hypoxic mice, as compared with normoxic values of 18 ± 2 mmHg and 19 ± 1 mmHg, respectively). Although our data are qualitatively consistent with previous experiments, there is a quantitative difference that may be explained based on the following. The mice we studied were on a homozygous C57BL/6 background, whereas mice used in previous experiments were on a hybrid background (SV129/C57BL/6) (25). There is also evidence that CO can modulate eNOS activity and expression (26).

Our data suggest that CO and NO work together to exert protective therapeutic effects to restore homeostasis. What is unclear is which of these two gases directly exerts the therapeutic effect, if indeed one of them does (perhaps the combination is required to achieve the beneficial effect). Our data in this study suggest that the effect of CO administration is dependent on eNOS and NO production for its salutary effects. In a recent study of the effects of CO in a model of hepatitis induced by TNF-α and D-galactosamine, we found a more complicated series of responses. In order for CO to act, it was necessary to have up-regulation of iNOS, production of NO, and, subsequently, induction of HO-1. Without each of these steps, CO (or NO given directly) had no effect (27).

NO is one of the most potent inducers of HO-1. It is thus unclear in the present model of PAH whether the effects of NO produced as a consequence of eNOS induction stimulated by CO are mediated directly or via HO-1. Likewise, in a model of carotid artery injury in which NO has been shown to be protective against intimal proliferation, protection conferred by NO is dependent on HO-1 (unpublished data). The enzymatic sources of NO are different in the liver model and in the present PAH model (i.e., iNOS and eNOS, respectively). In both cases, however, what is needed to mediate the effects of CO is NO, and in each case the organ and cell responds to provide that second gas. Perhaps these differences reflect the mode of injury and/or cell or tissue specificity. The fact that CO differentially regulates the generation of NO in different tissues, but in each to the benefit of the cells in that tissue, suggests that CO is a component of the natural protective system in those organs. Future studies continue to focus on understanding this complex relationship between CO and NO in terms of cellular and tissue cytoprotection.

The relative roles of CO and NO in PAH are interesting and, once again, quite interrelated. The progressive vascular hyperplasia that occurs in PAH involves both increased PAVSM cell proliferation and decreased regulation of cellular apoptosis (28). To reverse established PAH, the arterial wall must undergo some degree of negative remodeling to diminish pulmonary arterial hyperplasia and associated RVH. Our

co-culture results point to the necessity of cell–cell proximity, as CO exerted different effects in this system versus that observed in single cell preparations (Fig. 5). The ability of CO to induce cell death of the PAVSM cells only in the presence of PAECs, which are in part NO dependent, makes clear the complex interrelationship between these cell types and gas molecules. In addition, the important differences that arise in cell culture methodologies is critical when comparing with the in vivo setting.

Regression of hyperplasia occurs when the balance shifts toward decreased proliferation and increased apoptosis in the vessel wall. The role of NO in decreasing smooth muscle cell proliferation and migration, as well as inhibiting platelet aggregation, is well described (28–30). Similarly, CO suppresses platelet aggregation and smooth muscle cell proliferation, although the effects of migration are not known. There is certainly a distinct possibility that CO acts in part to suppress thrombogenesis and explains in part the therapeutic efficacy of CO in remodeling the pulmonary vasculature. CO exposure has no acute effect in reducing mPAP in normal rodents and sheep, which is not surprising because it is a relatively weak vasodilator, especially compared with NO. Although CO is not beneficial as an acute vasodilator, it acts importantly to reverse pulmonary artery and RV hypertrophy, acting as a therapeutic. NO inhalation is ineffective in treating adult pulmonary hypertension but acts rapidly and remarkably to alleviate neonatal hypertension (29). Perhaps the differences of responsiveness and age reflect etiological or disease progression differences.

NO thus clearly plays a role in the effects observed with CO. Although the concentrations of the NO donor required in vitro to induce cell death of PAVSM cells were high compared with that generated endogenously via the NOSes, we argue that perhaps the amount of NO produced by NOS in the microenvironment surrounding the juxtaposed endothelial and PAVSM cells allows for very high NO generation and exposure. Furthermore, the endogenous NO generated might be augmented in the presence of CO such that high intracellular concentrations could be achieved. We speculate that the effects of CO are pleiotropic in nature, acting directly on PAVSM cells to decrease proliferation and diminish inflammation, as well as acting on PAECs to decrease cellular injury. That CO also increases levels of endothelial NO, which diminishes pulmonary vascular hyperplasia by decreasing PAVSM cell mass via inhibition of proliferation and induction of apoptosis, may be an additional factor over and above those just discussed. Our data in the co-culture system speak to the necessity of the cell types being juxtaposed and interdigitated to some degree to allow adequate exposure to the gases and, most likely, other contributing factors such as immunomodulatory cytokines and mediators.

The primary goal of these experiments was to determine whether CO could treat PAH in a manner that is clinically relevant; we believe our results support such a notion. These data are the first to show that CO can act therapeutically in a clinically relevant disease model. Moreover, using the regimen of 1 h/d represents a reasonable clinical option. It should be noted that lower concentrations and shorter exposure times have not been tested.

How much CO is delivered to the pulmonary artery and right heart tissue by inhalation is unknown and difficult to measure reliably with present technology. CO bound to hemoglobin has an off rate that presumably helps to determine the amount of CO that would reach the pulmonary artery and right heart and target eNOS in the PAECs. The high diffusion and nonreactivity of CO must also be factored into CO delivery and exposure.

In summary, using three different models of pulmonary hypertension and right heart hypertrophy, we show the following. First, that a low (250 ppm) and short (1 h) daily CO exposure regimen can reverse established hypertension, resulting in near normal pressures and heart weights. Second, that this occurs in part via suppressing growth and increasing apoptosis of the vascular smooth muscle cells of the pulmonary artery. Third, that the ability of CO to exert its remodeling effects requires the expression and function of eNOS/NOS3 (31). Finally, that NO acts in part as the effector molecule to induce cell death of PAVSM cells while preserving the endothelial cells. We speculate that the NO that is generated acts in part to correct endothelial cell dysfunction that then leads to apoptosis of the dysregulated, hyperproliferative smooth muscle cells. Collectively, we demonstrate that CO and NO act in concert to exert beneficial effects in the cardiopulmonary system and reverse established pathology, and show for the first time that CO can act therapeutically. Is it possible that a combination gas therapy can be used? Exposure to inhaled NO to act as an acute pulmonary vasodilator initially, followed by intermittent exposure to CO, such as demonstrated in this paper, to reverse the pathology could perhaps be a potential therapeutic regimen. Currently there are limited alternatives for treatment of PAH (1). A recent report showed some success in treatment of PAH with a gene therapy approach to block prosurvival factors such as survivin, but using this clinically may prove difficult (32). The regimen of CO exposure we present is clinically feasible and could prove to be a useful therapy in the treatment of PAH.

MATERIALS AND METHODS

Animal models. The therapeutic exposure regimens for the MCT and chronic hypoxia models are depicted in Fig. 6. All animal protocols were approved by the animal care and use committee at the University of Pittsburgh School of Medicine and Beth Israel Deaconess Medical Center. Animals were allowed to acclimate 1 wk before experimentation with food and water ad libitum.

MCT. MCT (Sigma-Aldrich), dissolved in 1 N HCl neutralized with 0.5 N NaOH and diluted with PBS, was given as a single 50-mg/kg s.c. injection to male Sprague-Dawley rats weighing between 250 and 260g (Harlan), whereas control rats were injected with the same volume of saline. 250 ppm CO was administered for 2 wk at 1 h/d for the indicated time interval (Fig. 6).

Chronic hypoxia. Male Sprague Dawley rats were purchased from Harlan and allowed to acclimate for 1 wk with access to food and water ad libitum. Animals were placed in an airtight plexiglass chamber and exposed to 10%
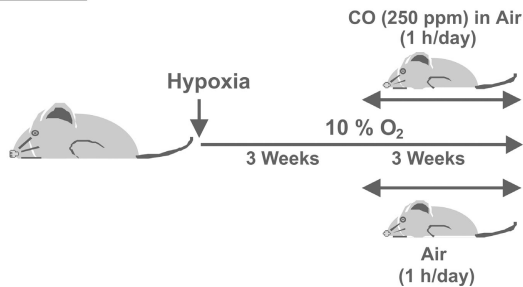
Monocrotaline
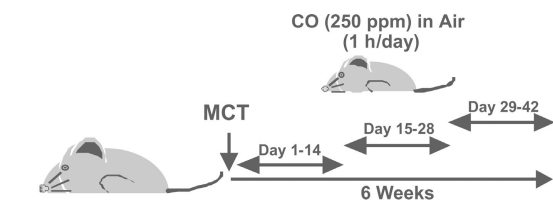
Hypoxia

Figure 6. Animal models. Pictorials depict MCT and hypoxia models with CO exposure regimes.

O_2 continuously for 6 wk. 3 wk into the exposure, rats were removed and placed in another airtight chamber and exposed to 250 ppm CO (in the air) or air (controls) for 1 h and then immediately returned to the 10% O_2 chamber (see Fig. 6). In vivo CO exposures were performed as previously described (7). This was repeated daily for the remaining 3 wk. PAH was determined on day 42. For the mouse hypoxia experiments, male C57BL6/J and $enos^{-/-}/nos3^{-/-}$ mice were purchased from The Jackson Laboratory and allowed to acclimate for 1 wk. The mice were exposed in an identical manner as that of the rat. mRVP was measured on day 42.

Male FHH rats (Charles River Laboratories) at 10 wk of age weighing ~250–300g were purchased and allowed to acclimate 2 wk before experimentation. FHH rats at this age are known to exhibit PAH. We then started CO exposure (250ppm for 1h/d) for a 3-wk duration and determined PAH after 3 wk. All animal protocols were approved by the University of Pittsburgh School of Medicine Animal Care and Use Committee.

Determination of PAH. At the end of the experiment, the animals were anesthetized, and RV pressures were measured using a fluid-filled pressure transducer connected to a PC-driven PowerLab (ADInstruments). Animal body weights were also measured before and after all treatments. Hearts and lungs were then harvested, the hearts were dissected, and the mass of the RV and LV plus IVS was measured. Sections of the lung and heart were fixed in 2% paraformaldehyde and snap frozen in liquid N_2. 7-μm sections were then immunostained.

Pulmonary artery morphometrics. Paraffin-embedded lung sections were stained with hematoxylin and eosin. Images for arterioles were captured with a microscope digital camera system (Provus; Olympus), and arterial area was measured using an image analysis program (Metamorph 6.2; Universal Imaging Corp.). Percent wall thickness was calculated by the following formula: wall thickness (%) = area external − area internal/area external × 100, where area external and area internal are the areas bounded by external elastic lamina and the lumen, respectively. 10 vessels/rat of comparable size from the lungs of five different rats from both MCT control and CO-treated (days 29–42) groups were determined, as well as untreated controls.

Cell culture. PAECs and vascular smooth muscle cells were cultured in DMEM containing 10% FBS and 100 μg/ml gentamicin. Cells were ex-

posed to 250 ppm CO or air using a bioactive gas controlling system custom designed and built by Biospherix Ltd. To achieve a concentration of 250 ppm, 1% (10,000 ppm) CO (Lifegas Inc.) was mixed with 5% CO_2/20.8% O_2/74% N_2 and controlled by software (Anafaze; Watflow) on a computer (Dimension DIM2400; Dell).

Co-culture of PAVSM cells and PAECs. PAVSM cells at passages 2–5 were seeded on the underside of collagen-impregnated, 24-mm permeable support inserts (Transwell; Corning) and placed in the cell culture incubator for 2 h, after which PAECs at passages 3–6 were seeded on the upper compartment and flip side of support. The PAEC/PAVSM cell co-culture inserts were then placed in six-well plates with media on both the upper and lower compartments. The 400-mm membrane pore size was specifically chosen to allow for interdigitation of cell processes between the two compartments, as well as the exchange of media and soluble mediators. However, migration of either cell type is highly improbable. On the day of the experiment, the PAEC/PAVSM cell co-cultures were exposed for either 24 or 48 h to either hypoxia (1% O_2/5% CO_2/balance N_2), CO (250 ppm/5% CO_2/balance N_2), hypoxia plus CO, or 5% CO_2 in air. A separate group of cells were pretreated with 500 μM L-NAME (Sigma-Aldrich) for 1 h before exposures for 24 and 48 h to hypoxia/CO. L-NAME was added once daily. At the end of the experiment, cells were harvested by trypsinization and subjected to FACS analysis for cell viability. Cells were observed before harvest. Based on morphological characteristics, contamination of each side by the other cell type was confirmed.

PI staining was performed using standard techniques. In brief, forward and side scatter gates were set to include cells but to exclude debris. Excitation was set at 488 nm, and emission was recorded on a sensor for PI (575 ± 10 nm; FL2; Sigma-Aldrich). Cell cycle and DNA content were detected with PI. Each experimental set was performed five times, and the data were analyzed with software (CellQuest; BD Biosciences).

DAF fluorescence as a measure of intracellular production of NO. PAECs were incubated with air or 250 ppm CO for 5–15 min. Cells were loaded with 5 μM 4-amino-5-methylamino-2',7'-difluorofluorscein (DAFH-DA; Invitrogen) 15 min before the harvest time point. DAFH-DA is a selective flourophor for NO. Cells were then washed, resuspended in FACS buffer (PBS + 1% FBS), and intensity of fluorescence was read at 503 nm for excitation and at 529 nm for emission wavelength, respectively. Macrophages treated with PMA were used as a positive control (unpublished data).

Immunoblotting. Cell and tissue lysates were separated by SDS-PAGE and blotted as described previously (14). Blots were incubated with primary rabbit anti-eNOS or -iNOS (BD Biosciences). Membranes were then washed in TTBS and visualized using horseradish peroxidase (HRP)–conjugated antibody against rabbit or mouse IgG and the enhanced chemiluminescence reagents (GE Healthcare), as per the manufacturer's instructions. To confirm equal loading, blots were reprobed with mouse mAb targeting β-actin (Abcam Inc.).

Immunostaining. Expression of Ki67, eNOS, and activated caspase-3 were detected in 5-μm lung sections with antibodies from Cell Signaling. Protein expression was visualized with HRP-conjugated goat anti–mouse or goat anti–rabbit antibodies (Invitrogen). Apoptotic cells were detected using a kit from Chemicon to detect TUNEL-positive cells, according to the manufacturer's instructions, including negative control staining. Nuclei were visualized with DAPI (Sigma-Aldrich). Staining was visualized in a blinded fashion on a microscope (Axiovert; Carl Zeiss MicroImagin, Inc.). 8–10 images were captured at random from each animal. Cell counts, where indicated, were performed blinded and expressed as cells/HPF.

REFERENCES

1. Humbert, M., O. Sitbon, and G. Simonneau. 2004. Treatment of pulmonary arterial hypertension. *N. Engl. J. Med.* 351:1425–1436.

2. Mandegar, M., Y.C. Fung, W. Huang, C.V. Remillard, L.J. Rubin, and J.X. Yuan. 2004. Cellular and molecular mechanisms of pulmonary vascular remodeling: role in the development of pulmonary hypertension. *Microvasc. Res.* 68:75–103.

3. Pietra, G.G., F. Capron, S. Stewart, O. Leone, M. Humbert, I.M. Robbins, L.M. Reid, and R.M. Tuder. 2004. Pathologic assessment of vasculopathies in pulmonary hypertension. *J. Am. Coll. Cardiol.* 43:25S–32S.

4. Mandegar, M., P.A. Thistlethwaite, and J.X. Yuan. 2004. Molecular biology of primary pulmonary hypertension. *Cardiol. Clin.* 22:417–429.

5. Badesch, D.B., S.H. Abman, G.S. Ahearn, R.J. Barst, D.C. McCrory, G. Simonneau, and V.V. McLaughlin. 2004. Medical therapy for pulmonary arterial hypertension: ACCP evidence-based clinical practice guidelines. *Chest.* 126:35S–62S.

6. Giaid, A., and D. Saleh. 1995. Reduced expression of endothelial nitric oxide synthase in the lungs of patients with pulmonary hypertension. *N. Engl. J. Med.* 333:214–221.

7. Giaid, A., D. Saleh, M. Yanagisawa, and R.D. Forbes. 1995. Endothelin-1 immunoreactivity and mRNA in the transplanted human heart. *Transplantation.* 59:1308–1313.

8. Saleh, D., K. Furukawa, M.S. Tsao, A. Maghazachi, B. Corrin, M. Yanagisawa, P.J. Barnes, and A. Giaid. 1997. Elevated expression of endothelin-1 and endothelin-converting enzyme-1 in idiopathic pulmonary fibrosis: possible involvement of proinflammatory cytokines. *Am. J. Respir. Cell Mol. Biol.* 16:187–193.

9. Jeffery, T.K., and N.W. Morrell. 2002. Molecular and cellular basis of pulmonary vascular remodeling in pulmonary hypertension. *Prog. Cardiovasc. Dis.* 45:173–202.

10. Yet, S.F., M.A. Perrella, M.D. Layne, C.M. Hsieh, K. Maemura, L. Kobzik, P. Wiesel, H. Christou, S. Kourembanas, and M.E. Lee. 1999. Hypoxia induces severe right ventricular dilatation and infarction in heme oxygenase-1 null mice. *J. Clin. Invest.* 103:R23–R29.

11. Christou, H., T. Morita, C.M. Hsieh, H. Koike, B. Arkonac, M.A. Perrella, and S. Kourembanas. 2000. Prevention of hypoxia-induced pulmonary hypertension by enhancement of endogenous heme oxygenase-1 in the rat. *Circ. Res.* 86:1224–1229.

12. Minamino, T., H. Christou, C.M. Hsieh, Y. Liu, V. Dhawan, N.G. Abraham, M.A. Perrella, S.A. Mitsialis, and S. Kourembanas. 2001. Targeted expression of heme oxygenase-1 prevents the pulmonary inflammatory and vascular responses to hypoxia. *Proc. Natl. Acad. Sci. USA.* 98:8798–8803.

13. Otterbein, L.E., M.P. Soares, K. Yamashita, and F.H. Bach. 2003. Heme oxygenase-1: unleashing the protective properties of heme. *Trends Immunol.* 24:449–455.

14. Otterbein, L.E., B.S. Zuckerbraun, M. Haga, F. Liu, R. Song, A. Usheva, C. Stachulak, N. Bodyak, R.N. Smith, E. Csizmadia, et al. 2003. Carbon monoxide suppresses arteriosclerotic lesions associated with chronic graft rejection and with balloon injury. *Nat. Med.* 9:183–190.

15. Morita, T., S.A. Mitsialis, H. Koike, Y. Liu, and S. Kourembanas. 1997. Carbon monoxide controls the proliferation of hypoxic vascular smooth muscle cells. *J. Biol. Chem.* 272:32804–32809.

16. Kourembanas, S. 2002. Hypoxia and carbon monoxide in the vasculature. *Antioxid. Redox Signal.* 4:291–299.

17. Dubuis, E., M. Potier, R. Wang, and C. Vandier. 2005. Continuous inhalation of carbon monoxide attenuates hypoxic pulmonary hypertension development presumably through activation of BKCa channels. *Cardiovasc. Res.* 65:751–761.

18. Coburn, R.F., R.E. Forster, and P.B. Kane. 1965. Considerations of the physiological variables that determine the blood carboxyhemoglobin concentrations in man. *J. Clin. Invest.* 44:1899–1910.

19. Zakhary, R., S.P. Gaine, J.L. Dinerman, M. Ruat, N.A. Flavahan, and S.H. Snyder. 1996. Heme oxygenase 2: endothelial and neuronal localization and role in endothelium-dependent relaxation. *Proc. Natl. Acad. Sci. USA.* 93:795–798.

20. Naik, J.S., and B.R. Walker. 2003. Heme oxygenase-mediated vasodilation involves vascular smooth muscle cell hyperpolarization. *Am. J. Physiol. Heart Circ. Physiol.* 285:H220–H228.

21. Dubuis, E., M. Gautier, A. Melin, M. Rebocho, C. Girardin, P. Bonnet, and C. Vandier. 2002. Chronic carbon monoxide enhanced IbTx-sensitive currents in rat resistance pulmonary artery smooth muscle cells. *Am. J. Physiol. Lung Cell. Mol. Physiol.* 283:L120–L129.

22. Otterbein, L.E., and A.M. Choi. 2000. Heme oxygenase: colors of defense against cellular stress. *Am. J. Physiol. Lung Cell. Mol. Physiol.* 279:L1029–L1037.

23. Thakker-Varia, S., C.A. Tozzi, S. Chari, K. Tiku, and D.J. Riley. 1999. Isolation of differentially expressed genes in hypertensive pulmonary artery of rats. *Exp. Lung Res.* 25:689–699.

24. Solari, V., A.P. Piotrowska, and P. Puri. 2003. Expression of heme oxygenase-1 and endothelial nitric oxide synthase in the lung of newborns with congenital diaphragmatic hernia and persistent pulmonary hypertension. *J. Pediatr. Surg.* 38:808–813.

25. Steudel, W., F. Ichinose, P.L. Huang, W.E. Hurford, R.C. Jones, J.A. Bevan, M.C. Fishman, and W.M. Zapol. 1997. Pulmonary vasoconstriction and hypertension in mice with targeted disruption of the endothelial nitric oxide synthase (NOS 3) gene. *Circ. Res.* 81:34–41.

26. Fujimoto, H., M. Ohno, S. Ayabe, H. Kobayashi, N. Ishizaka, H. Kimura, K. Yoshida, and R. Nagai. 2004. Carbon monoxide protects against cardiac ischemia–reperfusion injury in vivo via MAPK and Akt–eNOS pathways. *Arterioscler. Thromb. Vasc. Biol.* 24:1848–1853.

27. Zuckerbraun, B.S., T.R. Billiar, S.L. Otterbein, P.K. Kim, F. Liu, A.M. Choi, F.H. Bach, and L.E. Otterbein. 2003. Carbon monoxide protects against liver failure through nitric oxide–induced heme oxygenase 1. *J. Exp. Med.* 198:1707–1716.

28. Humbert, M., N.W. Morrell, S.L. Archer, K.R. Stenmark, M.R. MacLean, I.M. Lang, B.W. Christman, E.K. Weir, O. Eickelberg, N.F. Voelkel, et al. 2004. Cellular and molecular pathobiology of pulmonary arterial hypertension. *J. Am. Coll. Cardiol.* 43:13S–24S.

29. Wessel, D.L., I. Adatia, L.J. Van Marter, J.E. Thompson, J.W. Kane, A.R. Stark, and S. Kourembanas. 1997. Improved oxygenation in a randomized trial of inhaled nitric oxide for persistent pulmonary hypertension of the newborn. *Pediatrics.* 100:E7.

30. Singh, S., and T.W. Evans. 1997. Nitric oxide, the biological mediator of the decade: fact or fiction? *Eur. Respir. J.* 10:699–707.

31. McQuillan, L.P., G.K. Leung, P.A. Marsden, S.K. Kostyk, and S. Kourembanas. 1994. Hypoxia inhibits expression of eNOS via transcriptional and posttranscriptional mechanisms. *Am. J. Physiol.* 267:H1921–H1927.

32. McMurtry, M.S., S.L. Archer, D.C. Altieri, S. Bonnet, A. Haromy, G. Harry, S. Bonnet, L. Puttagunta, and E.D. Michelakis. 2005. Gene therapy targeting survivin selectively induces pulmonary vascular apoptosis and reverses pulmonary arterial hypertension. *J. Clin. Invest.* 115:1479–1491.